Anal. Chem. **2010,** *82,* 7169–7177

Visual Detection of Single-Nucleotide Polymorphism with Hairpin Oligonucleotide-Functionalized Gold Nanoparticles

Yuqing He,[†,‡,§] Kang Zeng,[‡] Anant S. Gurung,[§] Meenu Baloda,[§] Hui Xu,[§] Xibao Zhang,*[,†] and Guodong Liu*[,§]

Department of Dermatology, Guangzhou Institute of Dermatology, Guangzhou 510095, China, Department of Dermatology, Nanfang Hospital, Southern Medical University, Guangzhou 510515, China, and Department of Chemistry and Biochemistry, North Dakota State University, Fargo, North Dakota 58105

We report a simple, fast, and sensitive approach for visual detection of single-nucleotide polymorphism (SNP) based on hairpin oligonucleotide-functionalized gold nanoparticle (HO−Au-NP) and lateral flow strip biosensor (LFSB). The results presented here expand on prior work (Mao, X.; Xu, H.; Zeng, Q.; Zeng, L.; Liu, G. *Chem. Commun.* 2009, 3065−3067.) by providing new approach to prepare HO−Au-NP conjugates with a deoxyadenosine triphosphate (dATP) blocker, which shortens the preparation time of the conjugates from 50 to 8 h and lowers the detection limit 500 times. A hairpin oligonucleotide modified with a thiol at the 5′-end and a biotin at the 3′-end was conjugated with Au-NP through a self-assembling process. Following a blocking step with dATP, the hairpin structure of HO and dATP embed the biotin groups, and make the biotin groups in close proximity to the Au-NP surface, leading to the biotins being "inactive". The strategy of detecting SNP depends on the unique molecular recognition properties of HO to the perfect-matched DNA and single-base-mismatched DNA to generate different quantities of "active" biotin groups on the Au-NP surface. After hybridization reactions, the Au-NPs associated with the activated biotins are captured on the test zone of LFSB via the specific reaction between the activated biotin and preimmobilized streptavidin. Accumulation of Au-NPs produces the characteristic red bands, enabling visual detection of SNP. The preparations of HO−Au-NP conjugates with dATP and the parameters of assay were optimized systematically, and the abilities of detecting SNP were examined in details. The current approach is capable of discriminating as low as 10 pM of perfect-matched DNA and single-base-mismatched DNA within 25 min without instrumentation. Moreover, the approach provides a lower background and higher selectivity compared to the current molecular beacon-based SNP detection. The protocol should facilitate the simple, fast, and cost-effective screening of important SNPs and could readily find wide applications in molecular diagnosis laboratories and in point-of-care testing (field testing).

Single-nucleotide polymorphisms (SNPs), which make up about 90% of human genetic variation, are regarded as potent molecular, genetic markers and valuable indicators for biomedical research, drug development, clinical diagnosis, and disease therapy.[1−4] Current methods for screening SNPs rely on a wide variety of probes, e.g., molecular beacons (MBs),[5,6] peptide nucleic acids,[7] gold-particle-labeled oligonucleotides,[8−10] and nucleic acid protocols (such as ligation,[11,12] primer extension,[13] or endonuclease digestion[14]), in connection with different detection platforms (e.g., fluorescence,[15,16] gel electrophoresis,[17,18] mass spectroscopy,[19,20] electrochemistry,[21−25] and microgravimetry[26]). Until now, there

* To whom correspondence should be addressed. Phone: +1 701 231 8697. Fax: +1 701 231 8831. E-mail: zxibao@126.com (X.Z.); guodong.liu@ndsu.edu (G.L.).

† Guangzhou Institute of Dermatology.

‡ Southern Medical University.

§ North Dakota State University.

(1) The International HapMap Consortium. *Nature* **2007**, *449*, 851−861.
(2) Scuteri, A.; Sanna, S.; Chen, W. M.; Uda, M.; Albai, G.; Strait, J. *PLoS Genet.* **2007**, *3*, e115.
(3) Shabo, A. *Curr. Opin. Mol. Ther.* **2008**, *10*, 267–272.
(4) Kim, S.; Misra, A. *Annu. Rev. Biomed. Eng.* **2007**, *9*, 289–320.
(5) Marras, S. A.; Kramer, F. R.; Tyagi, S. *Genet. Anal.* **1999**, *14*, 151–156.
(6) Barreiro, L. B.; Henriques, R.; Mhlanga, M. M. *Methods Mol. Biol.* **2009**, *578*, 255–276.
(7) Ross, P. L.; Lee, K.; Belgrader, P. *Anal. Chem.* **1997**, *69*, 4197–4202.
(8) Taton, T. A.; Mirkin, C. A.; Letsinger, R. L. *Science* **2000**, *289*, 1757–1760.
(9) Xue, X.; Xu, W.; Wang, F.; Liu, X. *J. Am. Chem. Soc.* **2009**, *131*, 11668–11669.
(10) Dubertret, B.; Calame, M.; Libchaber, A. J. *Nature* **2001**, *19*, 365–370.
(11) Toubanaki, D. K.; Christopoulos, T. K.; Ioannou, P. C.; Flordellis, C. S. *Anal. Chem.* **2009**, *81*, 218–224.
(12) Iannone, M. A.; Taylor, J. D.; Chen, J.; Li, M. S.; Rivers, P.; Slentz-Kesler, K. A.; Weiner, M. P. *Cytometry* **2000**, *39*, 131–140.
(13) Hoogendoorn, B.; Owen, M. J.; Oefner, P. J.; Williams, N.; Austin, J.; O'Donovan, M. C. *Hum. Genet.* **1999**, *104*, 89–93.
(14) Lyamichev, V.; Mast, A. L.; Hall, J. G.; Prudent, J. R.; Kaiser, M. W.; Takova, T.; Kwiatkowski, R. W.; Sander, T. J.; de Arruda, M.; Arco, D. A. *Nat. Biotechnol.* **1999**, *17*, 292–296.
(15) Okamoto, A.; Kanatani, K.; Saito, O. *J. Am. Chem. Soc.* **2004**, *126*, 8364–8365.
(16) Duan, X.; Liu, L.; Wang, S. *Biosens. Bioelectron.* **2009**, *24*, 2095–2099.
(17) Gaunt, T. R.; Hinks, L. J.; Rassoulian, H.; Day, I. N. *Nucleic Acids Res.* **2003**, *31*, E48.
(18) Brazill, S. A.; Hebert, N. E.; Kuhr, W. G. *Electrophoresis* **2003**, *24*, 2749–2757.
(19) Fei, Z.; Smith, L. M. *Rapid Commun. Mass Spectrom.* **2000**, *14*, 950–959.
(20) Tost, J.; Gut, I. G. *Mass Spectrom. Rev.* **2002**, *21*, 388–418.
(21) Hebert, N. E.; Brazill, S. A. *Lab Chip* **2003**, *3*, 241–247.
(22) Liu, G.; Lin, Y. *J. Am. Chem. Soc.* **2007**, *129*, 10394–10401.
(23) Liu, G.; Lee, T. M. H.; Wang, J. *J. Am. Chem. Soc.* **2005**, *127*, 38–39.
(24) Zhang, S.; Wu, Z.; Shen, G.; Yu, R. *Biosens. Bioelectron.* **2009**, *24*, 3201–3207.

10.1021/ac101275s
Published on Web 08/03/2010

has been no consensus for the best SNP detection in terms of SNP throughput, sample throughput, simplicity, robustness, and cost. Although they are sensitive and specific, many of these systems have features that limit their practical use, such as tedious assay processes,[22,23] the need for expensive instruments (e.g., mass spectrometer),[19,20] and the need for tight control over the experimental conditions (e.g., temperature).[11–14]

Recently, MBs have received considerable interest because of the inherent signaling mechanism by energy transfer and the high selectivity.[6,27,28] The unique stem−loop structure, fluorophore−quencher pair, and the capability to discriminate single-base mutation enable the simple, rapid, and sensitive detection of SNPs.[27] The MB-based SNP detection uses a genotype-discriminating strategy similar to the TaqMan method; although it offers a high specificity, there are still many challenges associated with the development of MB probes.[27] For example, the detection still needs expensive, dual-labeled primers; meanwhile, fluorophores result in a high fluorescence background and, thus, a decrease in the detection sensitivity.[29] Although these MB-based SNP detection methods show promise to overcome the disadvantages of conventional SNP detection methods, these protocols are not yet widely used in routine clinical settings. Additional efforts are thus needed to create more broadly applicable methods that would allow accurate, sensitive, rapid, and low-cost SNP identification.

Recently we reported hairpin oligonucleotide-functionalized gold nanoparticle (HO−Au-NP) as probes in dry reagent strip biosensor for DNA analysis.[30] The HO modified with a thiol at the 5′-end and a biotin at the 3′-end was conjugated with Au-NP through a self-assembling process in the presence of 11-mercaptoundecanol (MUD) blockers. The ability of discriminating single-base-mismatched and perfect-matched DNA was demonstrated preliminarily. However, the approach suffered a poor detection limit (0.5 nM) and long preparation time (more than 2 days) of the HO−Au-NP conjugates. Here, we expand our prior work by providing a new approach to prepare HO−Au-NP conjugates with a deoxyadenosine triphosphate (dATP) blocker, which shortens the preparation time of the conjugates from 50 to 8 h and lowers the detection limit 500 times. The preparation of HO−Au-NP and the parameters of assay were optimized systematically, and the abilities of detecting SNP with the current approach were examined in detail. Combining the different molecular recognition properties of HO to the perfect-matched DNA and single-base-mismatched DNA with the unique optical properties of Au-NP, the current approach is capable of discriminating as low as 10 pM of perfect-matched DNA and single-base-mismatched DNA within 25 min without instrumentation. The promising properties of the approach are reported in the following sections.

MATERIALS AND METHODS

Apparatus. The Airjet AJQ 3000 dispenser, Biojet BJQ 3000 dispenser, clamshell laminator, and the guillotine cutting module CM 4000 were from Biodot Ltd. (Irvine, CA). The DT1030 portable strip reader was purchased from Shanghai Goldbio Tech. Co., Ltd. (Shanghai, China).

Reagents. Streptavidin, $HAuCl_4$, sucrose, hydroxylamine, Tween 20, Triton X-100, trisodium citrate, deoxyadenosine triphosphate (dATP), 11-mercaptoundecanol (MUD), bovine serum albumin (BSA), sodium chloride−sodium citrate (SSC) buffer 20× concentrate (pH 7.0), and phosphate buffer saline (0.01 M PBS, pH 7.4) were purchased from Sigma-Aldrich. Glass fibers (GFCP000800), cellulose fiber sample pads (CF-SP001700), laminated cards (HF000MC100), and nitrocellulose membranes (HFB18004 and HFB 24004) were purchased from Millipore (Billerica, MA). Hairpin oligonucleotide, target DNA, and control DNA probe were obtained from Integrated DNA Technologies, Inc. (Coralville, IA). The oligonucleotide sequences were as follows:

HO probe: 5′-thio/MC6-D/ACA CGC TCA TCA AGC TTT AAC TCA TAG TGA GCG TGT/biotin-3′.

Perfect-matched DNA: 5′-ACG CTC ACT ATG AGT TAA AGC TTG-3′.

Single-base-mismatched DNA: 5′-ACG CTG ACT ATG AGT TAA AGC TTG-3′.

Noncomplementary DNA: 5′-ATG GCA TCG CTT AGC TGC CAG TAC ACT GAT TGA AGA CAT CAT AGT GCA GAC AAG CAT ATC-3′.

Control DNA probe (complementary with HO, dispensed on the control zone of the LFSB): 5′-biotin/ACG CTC ACT ATG AGT TAA AGC TTG CTG AAG-3′. All chemicals used in this study were analytical reagent grade. All other solutions were prepared with ultrapure (>18 MΩ) water from a Millipore Milli-Q water purification system (Billerica, MA).

Preparation of Au-NPs. Au-NPs with average diameter 15 ± 3.5 nm were prepared according to the reported methods with slight modifications.[31] All glassware used in this preparation was thoroughly cleaned in aqua regia (three parts HCl and one part HNO_3), rinsed in doubly distilled water, and oven-dried prior to use. In a 500 mL, round-bottom flask, 100 mL of 0.01% $HAuCl_4$ in doubly distilled water were brought to boil with vigorous stirring, followed by the addition of 4.5 mL of 1% trisodium citrate. The solution turned deep blue within 20 s, and the final color changed to wine-red after 60 s. Boiling was pursued for an additional 10 min; the heating source was removed, and the colloid solution was stirred for another 15 min. The resulting Au-NP solution was stored in dark bottles at 4 °C and used to prepare the HO−Au-NP conjugate. The resulting solution of Au-NPs was characterized by an absorption maximum at 520 nm.

Preparation of HO−Au-NP Conjugates. A HO modified with a thiol at its 5′-end and a biotin at the 3′-end was used to prepare HO−Au-NP conjugates. Two methods were employed in the current study. The first method followed our prior work,[30] in which HO was immobilized on the Au-NP surface by self-

(25) Di Giusto, D. A.; Wlassoff, W. A.; Giesebrecht, S.; Gooding, J. J.; King, G. C. *J. Am. Chem. Soc.* **2004**, *126*, 4120–4121.
(26) Patolsky, F.; Lichtenstein, A.; Willner, I. *Nat. Biotechnol.* **2001**, *19*, 253–257.
(27) Kim, Y.; Sohn, D.; Tan, W. *Int. J. Clin. Exp. Pathol.* **2008**, *1*, 105–116.
(28) Liu, C. W.; Lin, Y. W.; Huang, C. C.; Chang, H. T. *Biosens. Bioelectron.* **2009**, *24*, 2541–2546.
(29) Zheleznaya, L. A.; Kopein, D. S.; Rogulin, E. A.; Gubanov, S. I.; Matvienko, N. I. *Anal. Biochem.* **2006**, *348*, 123–126.
(30) Mao, X.; Xu, H.; Zeng, Q.; Zeng, L.; Liu, G. *Chem. Commun.* **2009**, 3065–3067.
(31) Mao, X.; Ma, Y.; Zhang, A.; Zhang, L.; Zeng, L.; Liu, G. *Anal. Chem.* **2009**, *81*, 1660–1668.

Scheme 1. Schematic Illustration of the Preparations of Hairpin Oligonucleotide-Functionalized Gold Nanoparticle Conjugates Based on 11-Mercaptoundecanol (method 1) and dATP (method 2) Blockers

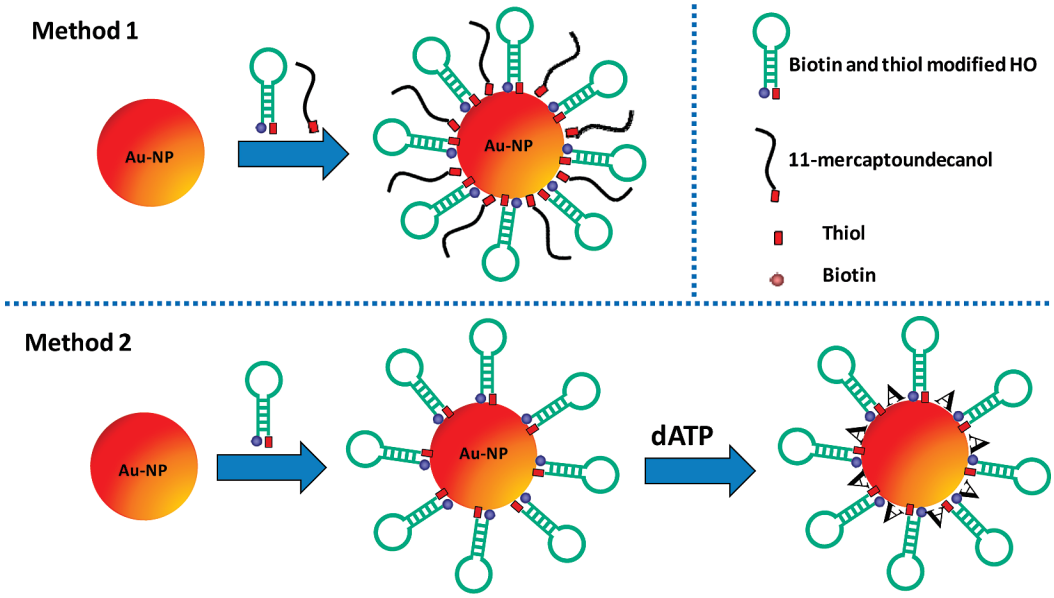

assembling in the presence of 11-mercaptoundecanol (Scheme 1, method 1). The second method was based on a dATP blocker (Scheme 1, method 2).

Method 1. The thiolated HO was first activated by the following procedure: 98 μL of thiolated HO (1.0 OD) was mixed with 2 μL of triethylamine and 7.7 mg of DTT to react for 30 min at room temperature (RT), then the excess DTT was removed by four times extraction with 400 μL of ethyl acetate solution. Conjugation reactions were carried out by adding 10 μL of 0.03 mM MUD and the activated HO to 1 mL of the 5-fold-concentrated Au-NP solution. After standing at 4 °C for 24 h, the solution was subjected to "aging" by the addition of NaCl up to a concentration of 150 mM, and a certain quantity of 1% SDS was added to reach a final concentration of 0.01%. The solution was allowed to stand for another 24 h at 4 °C, and the excess of reagents was removed by centrifugation for 20 min at 12 000 rpm. The supernatant was discarded, and the red pellet was redispersed in 1 mL of buffer containing 20 mM Na_3PO_4, 5% BSA, 0.25% Tween, and 10% sucrose.

Method 2. The thiolated HO probe (1.5 OD) was added to 1 mL of the 10-fold-concentrated Au-NP solution. After shaking 30 min at RT, 60 μL of 14.1 μM dATP was added to the solution and shook 15 min at RT. The HO−Au-NP conjugates were incubated for half an hour at RT and then put at 4 °C for 6 h to continue increasing the stability of the conjugate. The excess reagents were removed by centrifugation for 13 min at 12 000 rpm. After discarding the supernatant, the red pellets were washed twice with 0.01 M PBSB (pH 7.4, 1% BSA), recentrifuged, redispersed in 1 mL of an aqueous solution containing 20 mM $Na_3PO_4 \cdot 12H_2O$, 5% BSA, 0.25% Tween, and 10% sucrose, and stored at 4 °C before further use.

Preparation of the Lateral Flow Strip Biosensor (LFSB). The LFSB consists of four components: sample application pad, conjugate pad, nitrocellulose membrane, and absorbent pad (Supporting Information, Figure S1). The LFSB was assembled as described previously.[30,31] The test zone and control zone on the nitrocellulose membrane (25 mm ×30 cm) were prepared by dispensing a concentration of 1.25 mg mL^{-1} streptavidin and 1.25 mg mL^{-1} streptavidin−biotinylated DNA probe (control DNA probe, complementary with HO) solutions, respectively. The streptavidin−biotinylated DNA probes were prepared as described previously.[31] The solutions were then dispensed on the test and control zones of nitrocellulose membrane with the Biojet BJQ 3000 dispenser. The distance between the test zone and control zone was 2 mm. The membrane was then dried at 37 °C for 1 h and stored at 4 °C in a dry state. Finally, the sample pad, conjugate pad, nitrocellulose membrane, and absorption pad were assembled on a plastic adhesive backing (60 mm × 30 cm) using the clamshell laminator. Each part overlapped 2 mm to ensure the solution was migrating through the strip during the assay. Strips with a 3 mm width were cut by using the CM 4000 guillotine cutting module.

Analytical Procedure. Sample solutions containing various concentrations of target DNA (prefect-matched DNA, single-base-mismatched DNA, or noncomplementary DNA) were prepared in 4-fold-diluted SSC buffer containing 4% BSA. In a typical test, 100 μL of sample solution and 4 μL of HO−Au-NP conjugate solution were added to a 1.5 mL microcentrifuge tube; the mixture was incubated 5 min at RT. An LFSB was then dipped into the solution. After waiting for 10 min, 100 μL of running buffer (4-fold-diluted SSC buffer containing 4% BSA) was added to the microcentrifuge tube to wash the LFSB. The visual detection was completed in 10 min. The total assay time was 25 min. The intensities of the red bands on the test and control zones were determined by scanning the LFSB with a portable strip reader. Signal-to-noise (S/N) ratio of the assay was calculated by dividing the peak area of test band in the presence of DNA target by the peak area of test band in the absence of DNA target (control).

RESULTS AND DISCUSSION

Preparation of HO−Au-NP Conjugates with dATP Blockers. In the current study, the hairpin structure of HO and dATP blockers embed the biotin groups on the Au-NP surface and make it inactive. It is very important to use the blockers to block the leftover space of the Au-NP after the assembling of HO. The assembled blockers would reduce the nonspecific

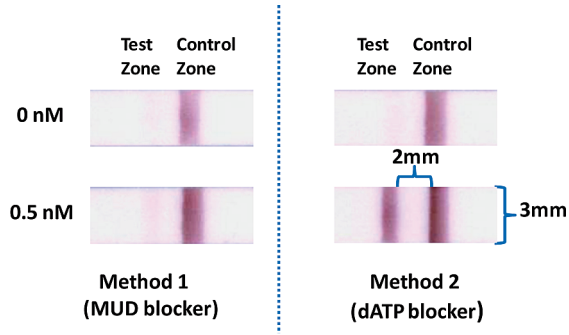

Figure 1. Typical photo images of LFSBs with the HO−Au-NP conjugates prepared with MUD (method 1) and dATP (method 2) blockers in the presence of 0 (control) and 0.5 nM perfect-matched DNA: assay time, 25 min; volume of HO−Au-NP, 4 μL; running buffer, 4× SSC + 4% BSA.

adsorption of HO−Au-NPs on the streptavidin surface in the test zone of the LFSB. An incomplete blocking would cause a high background. The blockers would also maintain the orientation of HO probes on the gold surface, resulting a high DNA hybridization efficiency. In our previous report,[30] The HO modified with a thiol at the 5′-end and a biotin at the 3′-end was conjugated with Au-NP via the self-assembled Au−S bond in the presence of 11-mercaptoundecanol (MUD) (Scheme 1, method 1). The hairpin structure of HO and the long carbon chain of MUD embed the biotin groups on the Au-NP surface and make it *inactive*. However, the visual detection limit of DNA (0.5 nM)[30] using this conjugate on the LFSB was relative high and similar with that using straight-chain oligonucleotide−Au-NP conjugates.[31] Furthermore, the preparation procedure, which was adapted from the conventional immobilization method of the thiolated oligonucleotides on the Au-NP surface, was tedious and took 2 days to complete.[30] In current study, HO−Au-NP conjugates were prepared by using dATP blocker (Scheme 1, method 2), which was used as a stabilizer to prepare DNA−Au-NP conjugates and shorten the preparation time of DNA−Au-NP.[32] The use of dATP blockers would shorten the preparation time of HO−Au-NP conjugates from 50 to 8 h, because dATP stabilized Au-NPs quickly in salt solution by forming a mononucleotide layer on particle surface and achieved a high DNA loading density. The high DNA density on the Au-NP surface is critical for the enhancement of DNA hybridization efficiency and the sensitivity of the assay. Briefly, the thiol- and biotin-modified HO was introduced to the Au-NP solution, and the mixture was incubated 30 min at RT. Following the addition of dATP, the mixture was incubated another 45 min at RT and then kept at 4 °C for 6 h to continue increasing the stability of the conjugate. The whole process took about 8 h to complete. We compared the analytical performances of two conjugates based on MUD and dATP blockers for the detection of perfect-matched DNA target. Figure 1 presents the photo images of LFSBs in the presence of 0 nM (control) and 0.5 nM perfect-matched DNA target. One can see that a weak red band was observed on the test zone of the LFSB with MUD blocker-based conjugates in the presence of 0.5 nM DNA target (method 1); a very bright red band was observed on the test zone of the LFSB with dATP blocker-based conjugates (method 2). Negligible signals were observed in the absence of DNA target (control) with both MUD- and dATP-based conjugates, indicating complete blocking with both blockers. The intensity of the band on the test zone of the LFSB with dATP-based conjugates is about 10 times higher than that with MUD-based conjugates. Such significant signal enhancement would be attributed to the different sizes of dATP and MUD. The size of MUD associated with a chain that has 11 carbons is much bigger than dATP. It could cause a steric hindrance which prevents some of the adsorbed HO from binding to target DNA and prevents the biotin groups from moving away from the Au-NP surface. The S/N ratio with dATP-based conjugates is 6 times higher than that with MUD-based conjugates.

Principle of Visual Detection for SNP. The principle of visual detection for SNP using HO−Au-NP and LFSB are illustrated in Scheme 2. It includes a hybridization reaction event between the target DNA and HO−Au-NP conjugate in a microcentrifuge tube (Scheme 2A) and an LFSB assay to capture the Au-NPs associated with activated biotin (Scheme 2B). The hybridization reactions of target DNA with the loop portions of the HOs on the Au-NP surface form a double-stranded structure and open the stem of the HO. Such confirmation change of HO pulls the biotin away from the Au-NP surface and then *activates* biotin, which exposes on the Au-NP surface and is able to react with streptavidin. The unique ability of HO in discriminating single-base-mismatched DNA and perfect-matched DNA results in the amount of *activated* biotin in the presence of single-base-mismatched DNA (Scheme 2A, I) being much less than that in the presence of perfect-matched DNA (Scheme 2A, II). In the cases of the presence of noncomplementary DNA (Scheme 2A, III) and the absence of perfect-matched DNA (Scheme 2A, IV), the HO on the Au-NP surface maintains its hairpin structure, and the biotin groups stay "inactive". The formed complexes are detected by an LFSB (Scheme 2B). The amount of captured Au-NPs in the test zone with a single-base-mismatched DNA sample solution is considerably less than that with a perfect-matched DNA sample solution because of fewer activated biotin groups. Therefore, the intensity of a red band on the test zone in the presence of single-base-mismatched DNA is significantly lower than that in the presence of perfect-matched DNA (Scheme 2B, I and II). Accordingly, in the case of an absence of perfect-matched DNA (control) and the presence of noncomplementary DNA, the biotin groups stay "inactive", and no Au-NP is captured on the test zone. In these cases, no red band is observed on the test zone (Scheme 2B, III and IV).

On the basis of the proposed approach, we tested the responses of four DNA samples. Figure 2 presents the typical photo images (Figure 2A) and corresponding optical responses (Figure 2B) of 0 nM perfect-matched DNA, 2.5 nM noncomplementary DNA, 2.5 nM single-base-mismatched DNA, and 2.5 nM perfect-matched DNA on LFSBs. As expected, no distinct red band was observed on the test zone of LFSBs in the absence of perfect-matched DNA and the presence of 2.5 nM noncomplementary DNA. A weak red band and a bright red band were observed on the test zones of LFSBs with 2.5 nM single-base-mismatched DNA and 2.5 nM perfect-matched DNA, respectively. The appearance of red bands in the test zone of

(32) Zhao, W.; Lin, L.; Hsing, I. *Bioconjugate Chem.* **2009**, *20*, 1218–1222.

Scheme 2. Schematic Illustration of the Principle of Visual Detection for Single-Nucleotide Polymorphism with Hairpin Oligonucleotide-Functionalized Gold Nanoparticles and a Lateral Flow Strip Biosensor: (A) Activating Biotin Groups through the Hybridization Events between Target DNA and Hairpin Oligonucleotides on Au-NPs; (B) Capturing Au-NPs on a Lateral Flow Strip Biosensor through Biotin−Streptavidin Interaction[a]

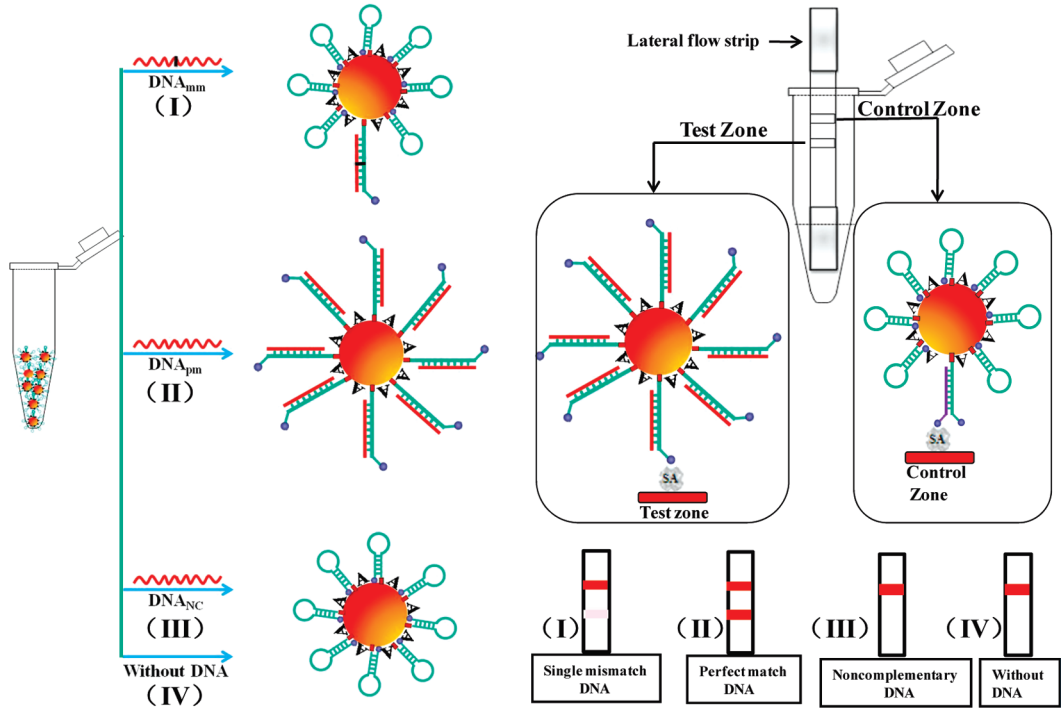

[a] DNA_{PM}, perfect-matched DNA; DNA_{MM}, single-base-mismatched DNA; DNA_{NC}, noncomplementary DNA.

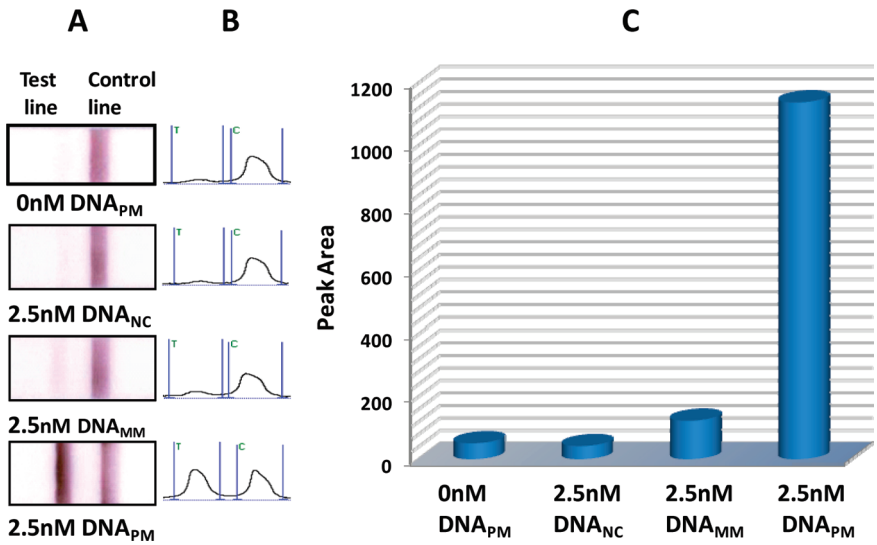

Figure 2. Typical photo images and corresponding optical responses of LFSB with 0 nM perfect-matched DNA (A), 2.5 nM noncomplementary DNA (B), 2.5 nM single-base-mismatched DNA and 2.5 nM perfect-matched DNA: assay time, 25 min; volume of HO−Au-NP, 4 μL; running buffer, 4× SSC + 4% BSA.

LFSB implied that the Au-NPs were captured on the test zone of LFSB through the interactions between the activated biotin groups and preimmobilized streptavidin. The color difference was ascribed to the different amounts of the captured Au-NPs in the test zone. In order to evaluate quantitatively, the intensities of the bands were recorded with a portable strip reader, and the signals are shown on the right side of each image (Figure 2B). The peak areas from the test zones were used for quantitative analysis. Figure 2C presents the histogram for the response of LFSB in the presence of different DNA sample solutions. It was found that the signal of single-base-mismatched DNA was only 10.8% of the perfect-matched DNA signal at this concentration level (2.5 nM). It indicated that the designed HO−Au-NP has excellent discrimination capability for perfect-matched DNA and single-base-mismatched DNA.

Optimization of the Preparation of HO−Au-NP Conjugates. *Effect of HO Concentration.* The amount of HO on the Au-NP surface would affect the hybridization efficiency of target DNA and HO. We studied the effect of the HO amount in the

self-assembling solution on the S/N ratio of the tests (Supporting Information, Figure S2A). Different amounts of HO ranging from 0.4 to 2.5 OD were mixed with 1 mL of 10-fold-concentrated Au-NP solution. The performance of the resulting conjugates was evaluated by detecting 0 and 1 nM perfect-matched target DNA. It was found that the S/N ratio increases upon raising the HO amount in the conjugate solution from 0.4 to 1.5 OD; further increasing the HO leads to decreases of the S/N ratio. The loss of the S/N ratio at a higher HO amount may be attributed to the formation of HO dimers or trimers in the conjugation solution because of base−base paring among HOs. The biotin groups associated with the absorbed dimers and trimers on the Au-NP surface may stay away from Au-NP surface and keep "active", thus leading to a high background signal and a low S/N ratio. Therefore, a 1.5 OD of HO in the conjugate solution was used to prepare the HO−Au-NP conjugates for the following experiments. The HO concentration in the resulted conjugate solution was determined with the reported method.[33] The number of HO per Au-NP was estimated to be 70 by dividing the number of HO with the number of Au-NPs.

Effect of dATP Concentration. In this study, dATP, a monomer unit of nucleic acid, was used as a blocker to prepare the HO−Au-NP conjugates. One of the functions of dATP is to block the leftover surface of the Au-NP after HO self-assembling. The absorbed dATP reduces the nonspecific HO binding and contributes to the right molecular orientation of the immobilized HO for hybridization.[32] Another function of dATP is to embed the biotin groups at the 3′-end of HO and make the biotin completely *inactive*, so the concentration of dATP would affect the performance of the HO−Au-NP conjugates. We studied the effect of dATP concentration on the S/N ratio of the tests by varying the dATP concentration in the conjugating solution (ranging from 7.05 to 28.2 μM). It was found that the S/N ratio increased upon raising the concentration of dATP from 7.05 to 14.1 μM; further increasing the concentration of dATP led to decreases of the S/N ratio (Supporting Information, Figure S2B). The signal of the control sample (in the absence of perfect-matched DNA) kept the constant value at a higher dATP concentration level; however, the signal of 1 nM perfect-matched DNA decreased. Such phenomena may be caused by the steric hindrance of dATP at high density on the Au-NP surface to prevent the biotin groups from moving away from the Au-NP surface. Therefore, a dATP concentration of 14.1 μM in the conjugate solution was used to prepare the HO−Au-NP conjugates for the following experiments.

Effect of the Self-Assembling Time. The self-assembling time of HO and dATP would affect the amount of HO and dATP absorbed on the Au-NP surface. Conventional self-assembling thiol-modified oligonucleotides on the Au-NPs were performed 2−3 days at 4 °C. Recent research showed that the use of dATP in the conjugation would accelerate the stabilization of the oligonucleotide−Au-NP conjugates and that the conjugation would be completed in a few hours.[32] In the current study, the conjugate solution was incubated for a short time period at room temperature after the addition of HO, dATP, SDS, and salts into the 10-fold-concentrated Au-NP solution and then put at 4 °C for 6 h to continue increasing the stability of the conjugates. It was found that the resulting conjugates showed equivalent or superior analytical performance compared to the conventional method (result not shown). We studied the effect of incubation time for the conjugate solution at room temperature on the S/N ratio of 1 nM perfect-matched DNA (Supporting Information, Figure S2C). It was found that the S/N ratio reached a maximum value at an incubation time of 30 min, followed by a gradual decrease at incubation times from 60 to 120 min. The results suggested that the short period of incubation at room temperature would help the adsorption of HO and dATP on the Au-NP surface and would reach an equilibrium state in a short time. Although a longer incubation time at room temperature would increase the absorption amount of HO and dATP, it may form some dATP aggregates on Au-NP surface, which have steric hindrance and prevent the biotin groups from moving away from the Au-NP surface. It would lead to a decreased signal and low S/N ratio. As a result, an incubation time of 30 min at room temperature was used for the following experiments.

Optimization of Assay Parameters. In the current study, HO−Au-NPs were used as probes for monitoring DNA hybridization events. The accumulations of Au-NPs on the test and control zones of the LFSB are visualized as characterized red bands which could be used for distinguishing perfect-matched DNA and single-base-mismatched DNA. The intensities of the red bands depend on the captured HO−Au-NP conjugates on the test and control zones which, in turn, correspond to the amount of conjugates on the reaction solution. To obtain a maximum response using a minimal amount of HO−Au-NP conjugates, the optimal amount of HO−Au-NP in the hybridization solution was estimated by incubating 1 nM perfect-matched DNA by increasing the volume of HO−Au-NP conjugates. It was found that the S/N ratio of the test increased up to 4 μL; a further increase of the volume caused a decrease of the S/N ratio (Supporting Information, Figure S3A), which was ascribed to an increased background signal; 4 μL of HO−Au-NP conjugates was routinely used for these assays.

Another factor to affect the sensitivity and reproducibility of the test is the amount of streptavidin, which is used to capture the formed biotin−DNA−DNA−Au-NP via a specific reaction between the activated biotin and streptavidin on the test zone of the LFSB. Streptavidin with different concentrations ranging from 0.5 to 2.0 mg mL^{-1} was used to prepare the test zone of the LFSB. The performance of the LFSBs was evaluated by detecting 0 and 1 nM perfect-matched DNA samples. The S/N ratio was found to be the highest for dispensing 1.25 mg mL^{-1} of streptavidin solution (Supporting Information, Figure S3B). The decrease in the S/N ratio at high concentration is ascribed to the increased background signal, which was caused by nonspecific adsorption of HO−Au-NP on the test zone. Therefore, 1.25 mg mL^{-1} of streptavidin solution was used to prepare the test zone of the LFSB in the following experiments.

Analytical Performance of SNP Discrimination. Under the optimal experimental conditions determined above, the ap-

(33) Demers, L. M.; Mirkin, C. A.; Mucic, R. C.; Reynolds, R. A.; Letsinger, R. L.; Elghanian, R.; Viswanadham, G. *Anal. Chem.* **2000**, *72*, 5535–5554.

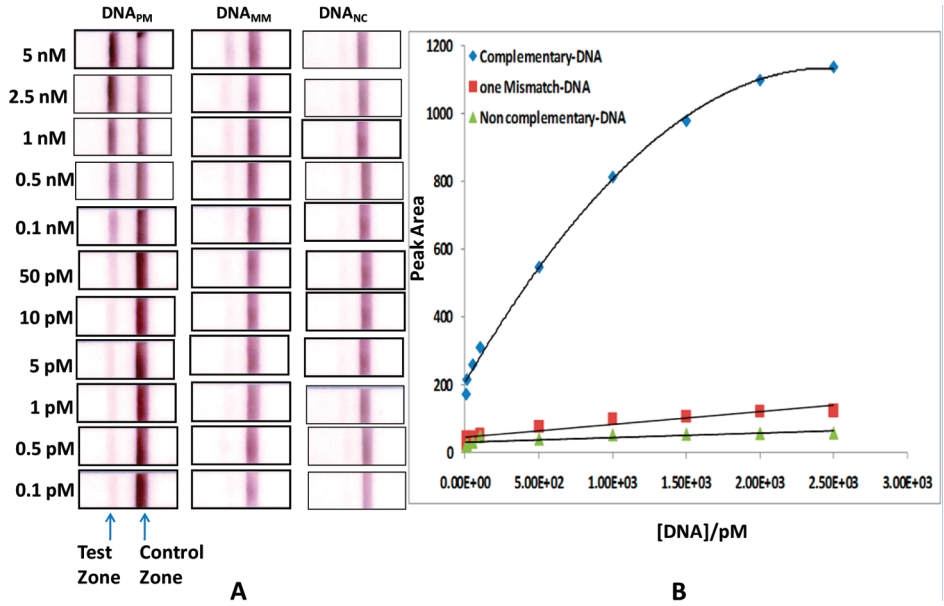

Figure 3. (A) Photo images of the LFSBs with different concentrations of perfect-matched DNA, single-base-mismatched DNA, and noncomplementary DNA; (B) the resulting calibration curves. The photo images and corresponding optical responses of red bands on the test zones of the LFSB were recorded with a strip reader. Other conditions are the same as in Figure 1.

proach was assessed for its analytical performance and ability to discriminate perfect-matched DNA, single-base-matched DNA, and noncomplementary DNA visually at different concentration levels ranging from 0.1 pM to 5.0 nM. The samples were analyzed on the LFSB, and images were subsequently recorded using the portable strip reader. The image was scanned across its length to convert the optical densities to digital values by employing "AuBio strip reader" software, and the values were then plotted against the position on the nitrocellulose membrane after normalization. Figure 3A presents the typical photo images of LFSBs in the presence of various target DNA with different concentrations. The resulting calibration plots of the peak areas versus target DNA concentrations are shown in Figure 3B. One can see that the intensities of the red bands on the test zones of LFSB are increasing with the increment of the concentrations of perfect-matched DNA and single-base-matched DNA (starting from 10 pM); one cannot discern the difference of the red bands in the test zones for concentrations of perfect-matched DNA between 0.1 and 10 pM. It would be caused by the fact that multiple HO probes were conjugated with one Au-NP (around 70 HO probes per Au-NP). At low concentration levels, multiple DNA targets may bind with one Au-NP through the hybridization events between the target DNA and HO on the Au-NP surface, and similar amounts of Au-NP labels were captured on the test zones of the strip biosensor, resulting in nondistinguishable red bands with naked eye. The reason is that people cannot discern more than ~100 shades of gray visually. Significant difference was observed between the perfect-matched DNA and one-mismatched DNA when the DNA concentration was more than 10 pM, which was used as the threshold for visually discriminating perfect-matched DNA and single-base-matched DNA. In addition, there is no red band observed on the test zones of the LFSBs in the presence of noncomplementary DNA even when the concentration of noncomplementary DNA is up to 2.5 nM, implying that noncomplementary DNA does not affect the detection.

Another benefit of current work is that the approach could be used for quantitative detection of perfect-matched DNA with the help of a strip reader. The calibration curve was prepared by plotting the peak areas versus logarithm of the DNA concentration (Supporting Information Figure S4). It should be mentioned that there was a linear relationship between the peak area and logarithm of the DNA concentration in the concentration range of 0.1−10 pM (Supporting Information, Figure S4A), in which the color was not distinguishable with the eye. We found that there were two linear ranges over the 0.1 pM to 2.5 nM range. The slope of in the range of 50 pM to 2.5 nM (see Figure S4B in the Supporting Information) is higher than that of the range of 0.1−10 pM (see Figure S4A in the Supporting Information). It may be attributed to the difference of hybridization reaction rates at these two concentration ranges. The quantitative detection limit of 0.1 pM (based on S/N = 3) perfect-matched DNA in SSC buffer was estimated in connection with the 25 min assay time. This detection of limit revealed 1000-fold[31] and 500-fold[30] improvements in sensitivity with the reported lateral flow nucleic acid biosensors in SSC buffer.

The selectivity is one of the most important parameters to evaluate the performance of SNP detection. In the current study, selectivity was obtained by dividing the intensity of the red band on the test zone from perfect-matched DNA (I_{PM}) by the intensity of the red band from single-base-mismatched DNA (I_{SM}). The intensities (peak area) of the red bands were recorded with a portable strip reader. It was found that the selectivity values almost kept a constant value of 9.0 at the concentration range of 0.1 pM to 1.0 nM. This value is much higher than the reported fluorescence-based MBs (4.0).[34]

(34) Taton, T. A.; Mirkin, C. A.; Letsinger, R. L. *Science* **2000**, *289*, 1757–1760.

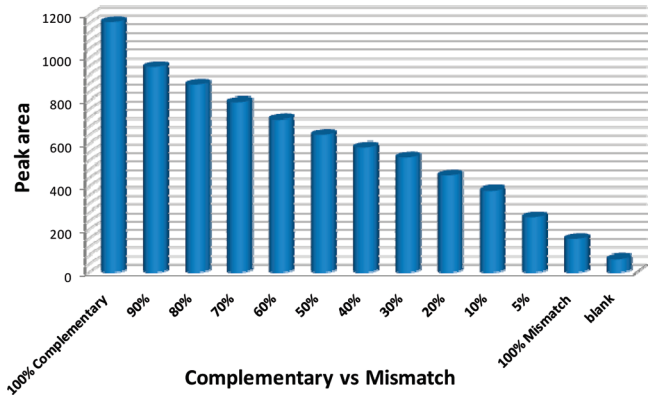

Figure 4. Effect of the wild-type (perfect-matched DNA) to mutant (single-base-mismatched DNA) ratio on the detection of SNP. The total concentration of DNA is 2.5 nM. Sample solutions were prepared by mixing perfect-matched DNA and single-base-mismatched DNA solution at different ratios. The volume of HO−Au-NP was 4 μL. Assay time: 25 min.

The selectivity values decreased at a higher DNA concentration. For example, the selectivity value was 4.3 with 5.0 nM DNA target. The decrease of the selectivity at a high concentration would be caused by the signal saturation of the perfect-matched DNA.

In order to further assess the specificity of our proposed approach, the wild-type target (perfect-matched DNA) and mutant target (single-base-mismatched DNA) were mixed together at different mole ratios with a total concentration of 2.5 nM. As shown in Figure 4, the intensity of the test line decreased with the increased mutant percentage in the sample solution. Obvious changes of the intensity can be observed even when the percentage of mutant in the samples is 10% (the single-base-mismatched DNA target concentration is about 0.25 nM), indicating that the proposed approach has excellent ability for detecting a scarce mutation among a large quantity of wild types.

Reproducibility is of significant importance in practical application for a visual judgment assay. The reproducibility of the current approach was assessed by testing 0 nM perfect-matched DNA (control), 1 nM perfect-matched DNA, 1 nM single-base-mismatched DNA, and 1 nM noncomplementary DNA. Figure 5 presents the photo images and corresponding optical responses of LFSBs. Each sample was tested six times with different LFSBs from the same batch preparation. One can see that similar responses were obtained for each tested sample. The coefficients of variation of the signals for the control, 1 nM perfect-matched DNA, 1 nM single-base-mismatched DNA, and 1 nM noncomplementary DNA were 6.4%, 4.0%, 7.7%, and 6.1%, respectively (n = 6). The overall relative standard deviation was less than 7.0%, which indicates a good reproducibility.

CONCLUSIONS

In the present work, we have demonstrated a simple, fast, and sensitive approach method for visual detection of SNP based on a hairpin oligonucleotide-functionalized gold nanoparticle and LFSB with high specificity and sensitivity. The strategy depends on the unique molecular recognition properties of HO to the perfect-matched DNA and single-base-mismatched DNA to generate different quantities of "active" biotin groups on the Au-NP surface. The preparation time of the conjugates was shortened from 50 to 8 h by using dATP blockers, and the detection limit was lowered 500 times compared with our prior work.[30] The procedure of detection is simplified by using Au-NP tracers and an LFSB which avoids the use of specialized instruments. Because of its simplicity, the assay does not require the training of highly qualified personnel. This approach provides a lower background and higher selectivity compared to the current molecular beacon based SNP detection. The selectivity value is up to 9.0. Current approach was capable of discriminating as low as 10 pM of perfect-matched DNA and single-base-mismatched DNA without instrumentation in 25 min. Further work will be targeted at the detection of SNP with genomic DNA samples and multiplex SNP detection. The protocol should facilitate the simple, fast, cost-effective screening of important SNPs and could readily find wide applications in molecular diagnosis laboratories and in point-of-care testing (field testing).

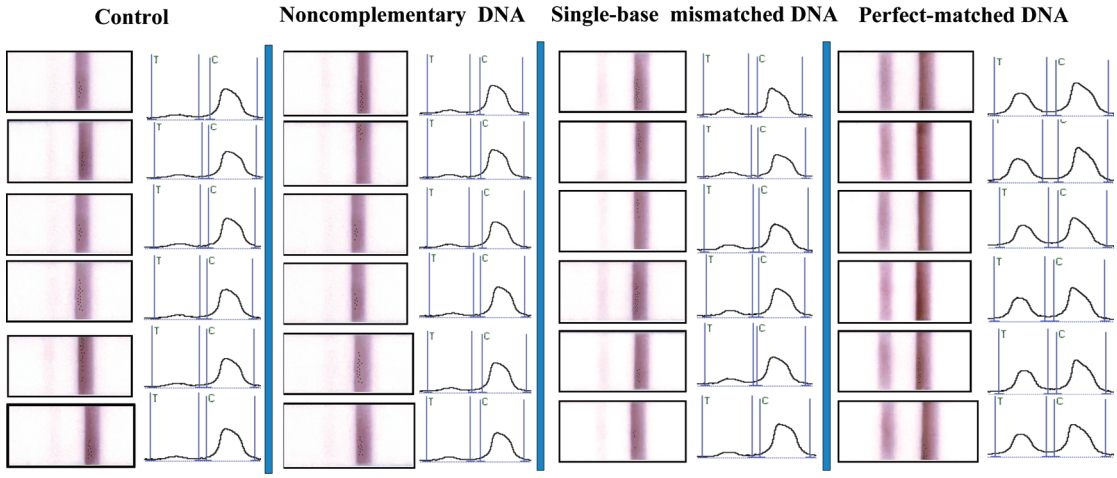

Figure 5. Photo images and corresponding optical responses of the LFSBs in the presence of 0 nM perfect-matched DNA (control), 1 nM noncomplementary DNA, 1 nM single-base-mismatched DNA, and 1 nM perfect-matched DNA. Tests were performed six times for each sample solution. Other conditions are the same as in Figure 4.

ACKNOWLEDGMENT

This research was supported by a Grant from the North Dakota Experimental Program to Stimulate Competitive Research (EPSCoR) and new faculty startup funds at North Dakota State University. Y. He acknowledges financial support from the Guangdong Provincial Natural Science Foundation of China (Nos. 06021655, 07001961, 07300648), the Key Research Plan of Guangzhou Health Department, China (No. 2006-ZDi-07), and the Guangdong Province Health Department Research Fund of China (No. A2007543).

NOTE ADDED AFTER ASAP PUBLICATION

This paper published on the web August 3, 2010 with incorrect graphics and captions for Figures 1 and 2. The revised version was published on August 6, 2010.

SUPPORTING INFORMATION AVAILABLE

Additional information as noted in text. This material is available free of charge via the Internet at http://pubs.acs.org.

Received for review March 3, 2010. Accepted July 8, 2010.

AC101275S